Fabrication of Double-Doped Magnetic Silica Nanospheres and Deposition of Thin Gold Layer

Sang-Eun Park, Jea-Won Lee,* Seung-Joo Haam,* and Sang-Wha Lee*

*Dept. of Chemical and Bio Engineering, Kyungwon University, Gyeonggi 461-701, Korea. *E-mail: lswha@kyungwon.ac.kr*
**Dept. of Chemical Engineering, Yonsei University, Seoul 120-749, Korea*
Received January 5, 2009, Accepted February 26, 2009

Double-doped magnetic particles that incorporated magnetites into both the surface and inside the silica cores were fabricated *via* the sol-gel reaction of citrate-stabilized magnetites with silicon alkoxide. Double-doped magnetic particles were easily fabricated and exhibited an higher magnetism in comparison to the single-doped magnetic particles that were prepared by the erosion of surface-deposited magneties from double-doped magentic particles. Thin gold layer was formed over magnetic silica nanospheres *via* nanoseed-mediated growth of gold clusters. The plasmon-derived absorption bands of double-doped magnetic silica-gold nanoshells were more broadened and shifted down by *ca.* 20 nm as compared to those of single-doped magnetic silica-gold nanoshells, which were attributed to not only the surface scattering of incident light due to relatively rough surafce morphology, but also heterogeneous permittivity of dielectric cores due to surface-deposited magnetites.

Key Words: Double-doped, Magnetites, Gold, Silica, Nanoshell

Introduction

Nanotechnology, one of the research frontiers in modern science and technology, has focused on the fabrication of hybrid nanostructures with unique optical and electromagnetic properties.[1,2] Gold nanoparticles can be an excellent candidate for biomedical applications owing to their unique optical properties along with biocompatible affinity for various functional ligands.[3,4] Halas and co-workers have reported that silica-gold nanoshells (SGNSs) successfully delivered a hyperthermic dose on the destruction of tumor cells *via* surface plasmon resonance (SPR) that is the collective oscillation of the conduction electrons confined in the metallic interface.[5,6]

The core-shell gold nanostructures combined with magnetic nanoparticles can provide a promising impact on simultaneous diagnostic imaging and targeted hyperthermia effect. In recent years, Diaz and other group reported SGNSs with magnetite-embedded in the silica cores.[7,8] Hyeon and co-worker also prepared silica-gold nanoshells (SGNSs) with magnetite-assembled on the silica cores.[9] The previous magnetic SGNSs used as a MRI (magnetic resonance imaging) and hyperthermia agent, however, exhibited relatively low contents of magnetites in silica matrix, probably due to single-doped magnetites either inside or outside the core. To ameliorate the detection sensitivity of MRI under the deteriorating biological medium, it is necessary to increase the contents of magnetites in the carrier medium or replace higher supermagnetic materials.

Most core-shell nanostructures were fabricated through the complex assembly process of small nanoparticles on ligand-functionalized oxide cores by electrostatic and/or chemical bonding. For instance, Mirkin *et al.* and other worker prepared the modified silica nanoparticle assembled with positively-charged amine groups for the attachment of negatively-charged Fe_3O_4 nanoparticles.[10,11] The water-in-oil (W/O) microemulsion has been used to synthesize the uniform magnetic materials, in which micelles (or inverse micelles) are used to control the thickness of silica layer on magnetic nanoparticles.[12] Core-shell gold composites were also prepared by a multistep (layer-by-layer, LBL) strategy based on the alternative assembly of oppositely-charged polyelectrolytes onto the colloidal templates.[7,13]

In contrast with the complex assembling process for single-doped magnetic nanoparticles, we reported the fabrication of double-doped magnetic silica nanospheres that incorporated magnetites onto both the inside and outside the core materials. Not only was the double-doped magnetic particles simply fabricated, but also exhibited an higher magnetism in comparison to the single-doped ones.[7-9] Thin gold layer was subsequently formed over magnetic silica nanospheres of which optical properties were influenced by surface morphology and heterogeneous dielectric cores. The facile fabrication of double-doped magnetic particles can be potentially applied to multi-functional magnetic systems such as nano-MRI, bio-analytic assays, and magnetic drug delivery.[2,14-16]

Experimental Section

Synthesis of magnetic silica nanospheres. To synthesize magnetic silica nanosphere, aqueous ferrofluid was prepared according to Massart's method.[17,18] $FeCl_3$ and $FeCl_2$ (3 : 2 mole ratio) were mixed with 25 mL of distilled water, and 20 mL of ammonium hydroxide (28 wt% NH_3) was added quickly to the chloride mixture under vigorous mechanical (nonmagnetic) stirring at room temperature. A black solid precipitate was immediately formed. The sediment was re-dispersed by ultrasonification in 50 mL of distilled water. Sodium citrate was subsequently added to magnetic ferrofluid and refluxed for 1 hour at 70 °C. Then, 0.5 mL of citrate-stabilized magnetites (15 g/L), 9.5 mL of H_2O, and 1.12 mL of NH_4OH were mixed in 40 mL ethanol, and then 0.5 mL tetraethyl orthosilicate (TEOS) solution was added to a mixed solution under mechanical stirring for 5~6 hours. Finally,

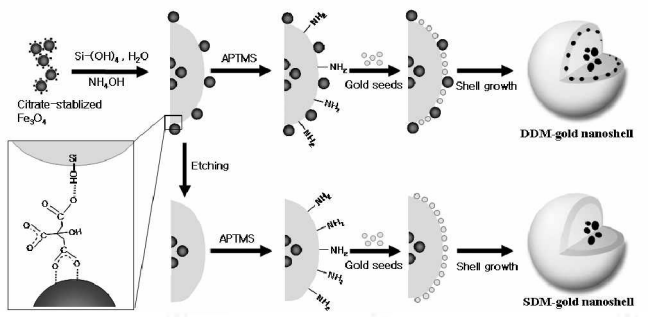

Figure 1. Schematic diagram of synthetic procedures for magnetic gold nanoshells with double-doped and single-doped magnetites.

double-doped magnetic silica nanospheres (Fe_3O_4@SiO_2-@Fe_3O_4) were obtained by sol-gel reaction of TEOS alkoxide with citrate-stabilized magnetites (CNMPs) in ethanol mixture.

Thin gold layer formation over magnetic silica nanospheres. To prepare gold colloids of 1~3 nm, tetrakis(hydroxymethyl) phosphonium chloride (THPC)/NaOH reducing agents were mixed with 1.0 wt% aqueous tetrachlroloaurate(III) trihydrate.[19] At the alkaline condition, THPC is a powerfully reducing agent enough to reduce gold salts *via* the derivation of formaldehyde. An excess of 3-aminopropyltrimethoxysilane (APTMS) was then added to a double-doped magnetic silica solution, and APTMS-functionalized magnetic particles were subsequently added to the gold colloids for the deposition of gold seeds onto the surface of magnetic nanoparticles. To form the continuous gold layer over the silica cores, gold-deposited magnetic nanoparticles (Au-Fe_3O_4@SiO_2@-Fe_3O_4) were further reduced by reacting with $K^+AuCl_4^-$ in the presence of formaldehyde.[6] Single-doped magnetic silica nanospheres were prepared by the erosion of surface-deposited magnetites in *conc.* HCl solution. Thin gold layer was also coated on the single-doped magnetic particles according to the same procedures that were previously described. Figure 1 describes the synthetic scheme for the fabrication of double-doped and single-doped magnetic silica nanospheres followed by the nanoseed-mediated growth of gold clusters.

Results and Discussion

Fe_3O_4 nanoparticles were prepared by co-precipitation of ferrous and ferric chlorides and the precipitates were processed in ultrasonic dispersion for DLS analysis. The magnetites obtained from the co-precipitation method exhibited a relatively wide distribution of particle sizes, 60 ± 37 nm. The agglomeration of magnetic nanoparticles provides challenges for them to be a building block for various functional nanocomposites. Thus, it is generally required to modify the surface of magnetites by inorganic and/or organic stabilizers.[20,21] In our case, citrate was employed as a surface-capping agent for Fe_3O_4 nanoparticles in order to prevent the agglomeration between magnetites. The size of citrate-capping magnetic nanoparticles (CMNPs) was significantly decreased down to 18 ± 5 nm, which indicated the stabilizing effect of citrate ions on the magnetic particles even though little has been understood about the interfacial coordination of citrate capping.[22]

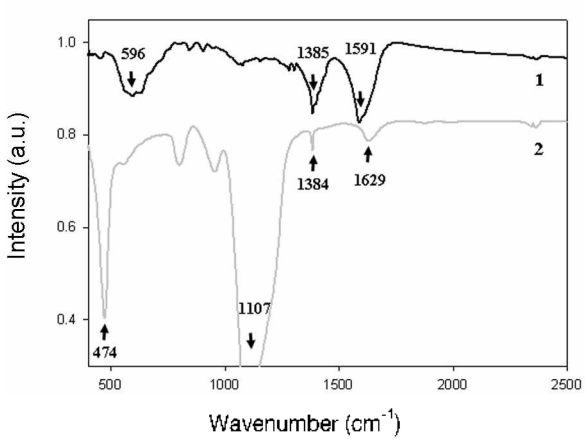

Figure 2. FTIR spectra of citrate-capped magnetites, 1, and citrate-capped magnetites deposited on silica nanospheres, 2.

In order to elucidate the anchoring effect of citrate-capped magnetites on the silica surface, pristine magnetites and citrate-capped magnetites were added into pure silica colloids prepared by the well-known Stöber method. TEM images clearly showed that only citrate-capped magnetites were attached onto silica nanospheres, but there was not any indication of pristine magnetites attached on the silica surface (data not shown). As shown in Figure 2, FTIR spectra of citrate-capped magnetites exhibited the characteristic peak of magnetites at 596 cm^{-1} and carboxylate groups of citrate at 1385 cm^{-1} and 1591 cm^{-1} that were assigned, respectively, to the symmetrical and asymmetrical stretching vibrations. Magnetite-deposited silica nanospheres also exhibited a strong silica peak at 1107 cm^{-1} and carboxylate groups at 1384 cm^{-1} and 1629 cm^{-1}, respectively. In contrast with the almost invariant position of symmetrical carboxylate peak, the asymmetrical carboxylate peak in magnetite-deposited silica was distinctly shifted to higher wave numbers by *ca.* 38 cm^{-1} as compared to that of citrate-capped magnetites. The reason may be that that hydrogen-mediated interaction between citrate carboxylates and silica hydroxyl groups render a more anisotropic distribution of electron density within magnetite-silica complexes, consequently leading to an upward shift of asymmetrical stretching bands of carboxylate groups.[23,24] At present, it is unclear whether the anchoring effect of citrate-capped magnetites is solely due to intermolecular interaction or to ligand exchange. FTIR spectrum analysis, however, suggested that anchoring effect of citrate-capped magnetites was contributed by the hydrogen-bonding interaction between carboxylate groups of citrate and hydroxyl groups of silica surface (see Figure 1).

Double-doped magnetic silica nanospheres (Fe_3O_4@SiO_2-@Fe_3O_4) were prepared by the modified sol-gel reaction of silicon alkoxide with excessive CMNPs, and single-doped magnetic silica nanospheres (Fe_3O_4@SiO_2) were obtained by etching the surface-exposed magnetites of double-doped magnetic particles in conc. HCl solution. As shown in Figure 3(a)-(b), the surface-deposited magnetites were clearly observed on the surface of silica nanospheres owing to the anchoring effect of citrate carboxylates that was previously

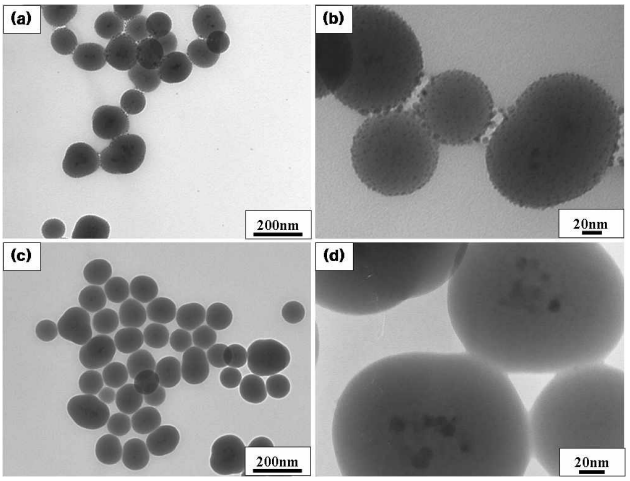

Figure 3. TEM images of magnetite-deposited silica nanospheres prepared by Stöber method of sol-gel reaction: (a) and (b) double-doped magnetites (DDM), (c) and (d) single-doped magnetites (SDM).

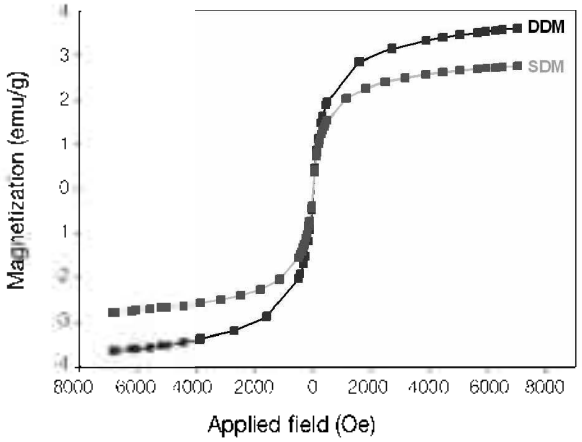

Figure 4. Hysteresis loops of magnetic silica nanospheres with DDM and SDM at 300 K, respectively.

described above. As shown in Figure 3(c)-(d), the aggregated magnetites were embedded inside the silica cores during the sol-gel reaction, which seemed to be attributed to the weakened stabilizing effect of deprotonated citrate carboxylates at high alkaline condition. Table 1 showed that double-doped magnetic (DDM) nanoparticles exhibited higher contents of Fe wt% and magnetism as compared to single-doped magnetic (SDM) nanoparticles, owing to the additional magnetites deposited outside the silica nanospheres. Figure 4 shows the hysteresis loops measured at 1.5 T (300 K) of silica nanospheres with double-doped and single-doped magnetites. Double-doped magnetic (DDM) particles exhibited a higher magnetism compared to single-doped magnetic (SDM) particles, probably due to the additional magnetites outside the silica nanospheres.

Magnetic silica nanospheres were self-assembled by APTMS having terminal amine groups that can give rise to positive zeta-potentials. In this case, the zeta-potential values were mainly determined by the numbers of amine groups exposed on magnetic particles. APTMS-modified magnetic

Table 1. The characteristics of gold-Fe_3O_4/*d*/silica nanocomposites

	Fe_3O_4 magnetites	Citrated-stabilized Fe_3O_4	Fe_3O_4/*d*/SiO_2 DDM	Fe_3O_4/*d*/SiO_2 SDM
Size (nm) by DLS[a]	60 ± 37	18 ± 5	140 ± 26	114 ± 25
Zeta-potential (mV)[b]	-33	-44	-57 (27)	-43 (33)
Fe wt% by EDX	–[c]	–[c]	2.5 wt%	1.13 wt%
emu/g[d]	80	46.1	3.6	2.7

[a]Size of nanoparticles were determined by intensity-based dynamic laser scattering (DLS) method in dilute condition of 3 10^{-4} g mL. [b]The zeta-potential of each nanoparticles in aqueous solution was measured in the neutral pH ranges (pH 7~8) and bracket number indicates the zeta-potential of APTMS-coated Fe_3O_4/*d*/SiO_2 in ethanol solution. [c]The Fe wt% can be estimated based on the stoichiometric composition of the iron oxide materials. [d]This represented saturated magnetization values by using a vibration sample magnetometer (VSM).

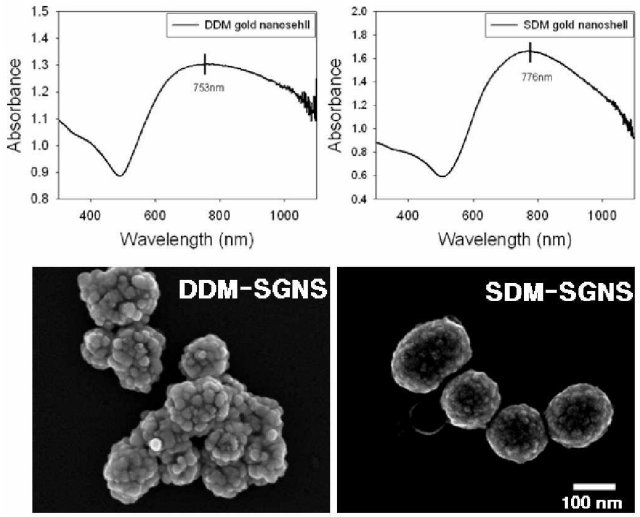

Figure 5. UV-Vis spectra of single-doped magnetic silica-gold nanoshells (SDM-SGNSs) and double-doped magnetic silica-gold nanoshells (DDM-SGNSs) (including SEM images), respectively.

SiO_2 exhibited the zeta-potential of +27 mV for double-doped magnetites and +33 mV for single-doped magnetites. The low zeta-potential values in double-doped magnetic nanoparticles indicated that surface-exposed magnetites partially screened the hydroxyl groups of silica nanosphere available for APTMS assembly, consequently reducing amine groups assembled on magnetic silica nanospheres. Au-deposited magnetic nanoparticles were subsequently obtained by the electrostatic attractions between gold colloids with negative surface charges and APTMS-assembled SiO_2 with positive surface charges. THPC/NaOH-induced gold colloids (1~3 nm) at *ca.* pH 3.0 led to monodisperse deposition of gold colloids onto silica nanospheres.[25] Thin gold layer was formed over magnetic silica nanospheres *via* seed-mediated growth of gold clusters in the presence of reducible gold salts, $KAuCl_4$, and formaldehyde reducing agents.

Figure 5 exhibited the SEM images of double-doped magnetic silica-gold nanoshells (DDM-SGNSs) and single-doped magnetic silica-gold nanoshells (SDM-SGNSs), respectively. The surface morphology of DDM-SGNSs was relatively rough because the coalescence between neigh-

bouring gold clusters were interfered by surface-deposited magnetites, whereas SDM-SGNS exhibited the smoother surface morphology of thin gold layers. The core radius and shell thickness of SDM-SGNS were determined as *ca.* 58 nm and *ca.* 21 nm, respectively. As shown in Figure 5, the absorption peak of DDM-SGNSs was relatively less intense than that of SDM-SGNSs. Maximal absorption peaks of DDM-SGNSs and SDM-SGNSs were positioned at *ca.* 753 nm and 776 nm, respectively. Since SPR is a resonant interaction between the electromagnetic field of incident light and the surface charge oscillation, rough surface of metal layer can raise the surface scattering of incident light with the consequent weakening of SPR.[26,27]

In summary, the plasmon-derived absorption bands of DDM-SGNSs were more broadened and shifted down by *ca.* 20 nm in comparison to those of SDM-SGNS, probably due to the large grain domains of gold clusters and heterogeneous permittivity of dielectric cores attributed to the surface-deposited magnetites.[28,29]

Conclusions

Double-doped magnetic silica-gold nanoshells (DDM-SGNSs) were facilely synthesized by the sol-gel process of citrate-stabilized magnetites (CMNPs) with silicon alkoxide, followed by the seed-mediated growth of gold clusters over magnetic silica nanospheres. The successful fabrication of double-doped magnetic silica nanospheres was mainly contributed by two key factors: i) magnetites were stabilized by citrate capping during the sol-gel process, ii) citrate carboxylates capped on magnetites also provided the anchoring effect on the surface of silica nanospheres *via* hydrogen-bonding interaction. Double-doped magnetic particles exhibited higher magnetism in comparison to single-doped magnetic particles. DDM-SGNSs exhibited a relatively rough surface morphology and large grain size owing to the interference of surface-deposited magnetites in the formation of thin gold layer, resulting in the blue-shift of absorption bands and the decrease of absorption intensity. This synthetic route for double-doped magnetic particles can provide a possible multiple-doped magnetic system *via* successive sol-gel reaction of citrate-stabilized magnetites with silicon alkoxide.

Acknowledgments. This work was supported by KOSEF grant funded by the Korea government (MOST) (200605382).

References

1. Eustis, S.; El-sayed, M. A. *Chem. Soc. Rev.* **2006**, *35*, 209.
2. Lu, A. H.; Salabas, E. L.; Schüth, F. *Angew. Chem. Int. Ed.* **2007**, *46*, 1222.
3. Daniel, M. C.; Astruc, D. *Chem. Rev.* **2004**, *104*, 293.
4. Brust, M.; Kiely, C. J. *Colloids and Surfaces A: Physicochemical and Engineering Aspects* **2002**, *202*, 175.
5. Hirsch, L. R.; Stafford, R. J.; Bankson, J. A.; Sershen, S. R.; Rivera, B.; Price, R. E.; Hazle, J. D.; Halas, N. J.; West, J. L. *PNAS* **2003**, *100*, 13549.
6. Pham, T; Jackson, J. B.; Halas, N. J.; Lee, T. R. *Langmuir* **2002**, *18*, 4915.
7. Maceira, V. S.; Duarte, M. A. C.; Farle, M.; Quintela, A. L.; Sieradzki, K.; Diaz, R. *Chem. Mater.* **2006**, *18*, 2701.
8. Ji, X.; Shao, R.; Elliott, A. M.; Stafford, R. J.; Coss, E. E.; Bankson, J. A.; Liang, G.; Luo, Z. P.; Park, K.; Markert, J. T.; Li, C. *J. Phys. Chem. C* **2007**, *111*, 6245.
9. Kim, J.; Park, S.; Lee, J. E.; Jin, S. M.; Lee, J. H.; Lee, I. S.; Yang, I.; Kim, J. S.; Kim, S. K.; Cho, M. H.; Hyeon, T. *Angew. Chem. Int. Ed.* **2006**, *45*, 7754.
10. Stoeva, S. I.; Huo, F.; Lee, J. S.; Papaefthymiou, G. C.; Kundaliya, D.; Ying, J. Y. *J. Am. Chem. Soc.* **2005**, *127*, 4990.
11. Barnakov, Y. A.; Yu, M. H.; Rosenzweig, Z. *Langmuir* **2005**, *21*, 7524.
12. Santra, S.; Tapec, R.; Theodoropoulou, N.; Dobson, J.; Hebard, A.; Tan, W. *Langmuir* **2001**, *17*, 2900.
13. Aliev, F. G.; Duarte, M. A. C.; Mamedov, A.; Ostrander, J. W.; Giersig, M.; Marzan, L. M. L.; Kotov, N. A. *Adv. Mater.* **1999**, *11*, 1006.
14. Sharma, P.; Brown, S.; Walter, G.; Santra, S.; Moudgil, B. *Adv. Colloid Interface Sci.* **2006**, *123*, 471.
15. Yang, J.; Lee, C.; Ko, H.; Suh, J.; Yoon, H.; Lee, K.; Huh, Y.; Haam, S. *Angew. Chem. Int. Ed.* **2007**, *46*, 8836.
16. Gupta, A. K.; Gupta, M. *Biomaterials* **2005**, *26*, 3995.
17. Massart, R. *IEE Trans. Magn.* **1981**, *12*, 1247.
18. Liu, X.; Ma, Z.; Xing, J.; Liu, H. *J. Magn. Mater.* **2004**, *270*, 1.
19. Duff, D. G.; Baiker, A. *Langmuir* **1993**, *9*, 2310.
20. Lu, Y.; Yin, Y.; Mayers, B. T.; Xia, Y. *Nano Lett.* **2002**, *2*, 183.
21. Li, T.; Deng, Y.; Song, X.; Jin, Z.; Zhang, Y. *Bull. Korean Chem. Soc.* **2003**, *24*, 957.
22. Morais, P. C.; Santos, R. L.; Pimenta, A. C. M.; Azevedo, R. B.; Lima, E. C. D. *Thin Solid Film* **2006**, *515*, 266.
23. Hay, M. B.; Myneni, S. C. B. *Geochim. Cosmochim. Acta* **2007**, *71*, 3518.
24. Lanigan, K. C.; Pidsosny, K. *Vib. Spectrosc.* **2007**, *45*, 2.
25. Park, S. E.; Park, M. Y.; Han, P. K.; Lee, S. W. *Bull. Korean Chem. Soc.* **2006**, *27*, 1341.
26. Barnes, W. L.; Dereux, A.; Ebbesen, T. W. *Nature* **2003**, *424*, 824.
27. Raether, H. *Surface Plasmons*; Springer: Berlin, 1988; p 36.
28. Jung, Y. S.; Sun, Z.; Blachere, J.; Kim, H. K. *Appl. Phys. Lett.* **2005**, *87*, 263116.
29. Miller, M. M.; Lazarides, A. A. *J. Phys. Chem. B* **2005**, *109*, 21556.